Towards Ruthenium(II)-Rhenium(I) Binuclear Complexes as Photosensitizers for Photodynamic Therapy

Wang, Youchao ; Felder, Patrick S ; Mesdom, Pierre ; Blacque, Olivier ; Mindt, Thomas L ; Cariou, Kevin ; Gasser, Gilles

DOI: https://doi.org/10.1002/cbic.202300467

ChemBioChem

Research Article
doi.org/10.1002/cbic.202300467

Chemistry Europe
European Chemical Societies Publishing

www.chembiochem.org

Special Collection

Towards Ruthenium(II)-Rhenium(I) Binuclear Complexes as Photosensitizers for Photodynamic Therapy

Youchao Wang[+],[a] Patrick S. Felder[+],[a] Pierre Mesdom,[a] Olivier Blacque,[b] Thomas L. Mindt,[c, d, e] Kevin Cariou,*[a] and Gilles Gasser*[a]

The search for new metal-based photosensitizers (PSs) for anticancer photodynamic therapy (PDT) is a fast-developing field of research. Knowing that polymetallic complexes bear a high potential as PDT PSs, in this study, we aimed at combining the known photophysical properties of a rhenium(I) tricarbonyl complex and a ruthenium(II) polypyridyl complex to prepare a ruthenium-rhenium binuclear complex that could act as a PS for anticancer PDT. Herein, we present the synthesis and characterization of such a system and discuss its stability in aqueous solution. In addition, one of our complexes prepared, which localized in mitochondria, was found to have some degree of selectivity towards two types of cancerous cells: human lung carcinoma A549 and human colon colorectal adenocarcinoma HT29, with interesting photo-index (PI) values of 135.1 and 256.4, respectively, compared to noncancerous retinal pigment epithelium RPE1 cells (22.4).

Introduction

Photodynamic therapy (PDT) is a minimally invasive tumor treatment approach based on the use of a photosensitizer (PS) that is irradiated at a precise wavelength corresponding to the absorption band of the PS. After activation, the PS transfers its energy to molecular oxygen ($^3O_2$) to form toxic singlet oxygen ($^1O_2$), leading to tumor cell death.[1] While most of the PDT PSs used in the clinics are metal-free, some metal-based PSs are used in the clinics or are currently tested in clinical trials.[2–3] Ruthenium polypyridyl complexes are a promising class of compounds as PDT PSs.[4–5] TLD 1433 is the most successful representative of this class and has entered Phase II clinical trials against bladder cancer.[6] A significant advantage of metal complexes over classical organic-based PS such as Photofrin or Hematoporphyrin (HpD) is their singlet oxygen production efficiency.[7] Transition metal complexes often benefit from relativistic heavy atom effects. The transition from an excited singlet state (S_1) to a triplet state (T_1), the so-called inter-system crossing (ISC), is spin-forbidden and therefore unlikely and slow. Spin-orbit coupling (SOC), a phenomenon that occurs in heavy elements, significantly increases the probability of ISC.[8] Therefore, in order to increase the tendency for ISC of organic-based PSs, a common strategy is to place heavy atoms close to them.[9–12]

Rhenium(I) tricarbonyl complexes were found to be potential chemotherapeutic agents against cancer many years ago, several compounds have demonstrated cytotoxicity that matches or surpasses that of cisplatin, a clinically used anticancer drug.[13–17] In addition, Re(I) tricarbonyl complexes were found to be efficient PDT PSs.[18–19] For these reasons, the combination of a Ru(II) polypyridyl complex and a Re(I) tricarbonyl complex in a single molecule would be beneficial for the design of a PDT PS as it would give a high probability for ISC. Many bimetallic Ru(II)-Re(I) complexes were reported to possess the ability of intramolecular energy transfer.[20–22] For example, $Re(CO)_3Cl$-based Ru complex (**I**) showed that the energy transfer from Re to Ru takes place with nearly 100% efficiency (Figure 1).[23] $Re(bpy)(CO)_3$-based Ru compound (**II**) exhibited long-lived photoinduced charge-separated states.[24] Another $Re(bpy)(CO)_3$-based Ru compound (**III**) demonstrated that the combination of Ru and Re could change photophysical characteristics of the original Ru compound. Moreover, The excited state energy transfer from the Re(I) chromophore to the Ru(II) was observed.[25] To date, these compounds normally used bisimine ligands such as bipyridine along with halogen-bound element (Cl) or a single ligand (pyridine derivatives),

[a] *Y. Wang,[+] Dr. P. S. Felder,[+] Dr. P. Mesdom, Dr. K. Cariou, Prof. Dr. G. Gasser*
Chimie ParisTech, PSL University, CNRS, Institute of Chemistry for Life and Health Sciences, Laboratory for Inorganic Chemical Biology
75005 Paris (France)
E-mail: kevin.cariou@chimieparistech.psl.eu
gilles.gasser@chimieparistech.psl.eu

[b] *Dr. O. Blacque*
University of Zurich, Department of Chemistry,
CH-8057Zurich (Switzerland)

[c] *Prof. Dr. T. L. Mindt*
Institute of Inorganic Chemistry
Faculty of Chemistry, University of Vienna
Währingerstraße 42, 1090 Vienna (Austria)

[d] *Prof. Dr. T. L. Mindt*
Joint Applied Medicinal Radiochemistry Facility
University of Vienna
Währingerstraße 42, 1090 Vienna (Austria)

[e] *Prof. Dr. T. L. Mindt*
Medical University of Vienna
Währinger Gürtel 18–20, 1090 Vienna (Austria)

[+] *These authors contributed equally to this work.*

Supporting information for this article is available on the WWW under https://doi.org/10.1002/cbic.202300467

Special Collection *This article is part of the SCF-ChemBio: Chemical Biology Tour de France Special Collection. Please see our homepage for more articles in the collection.*

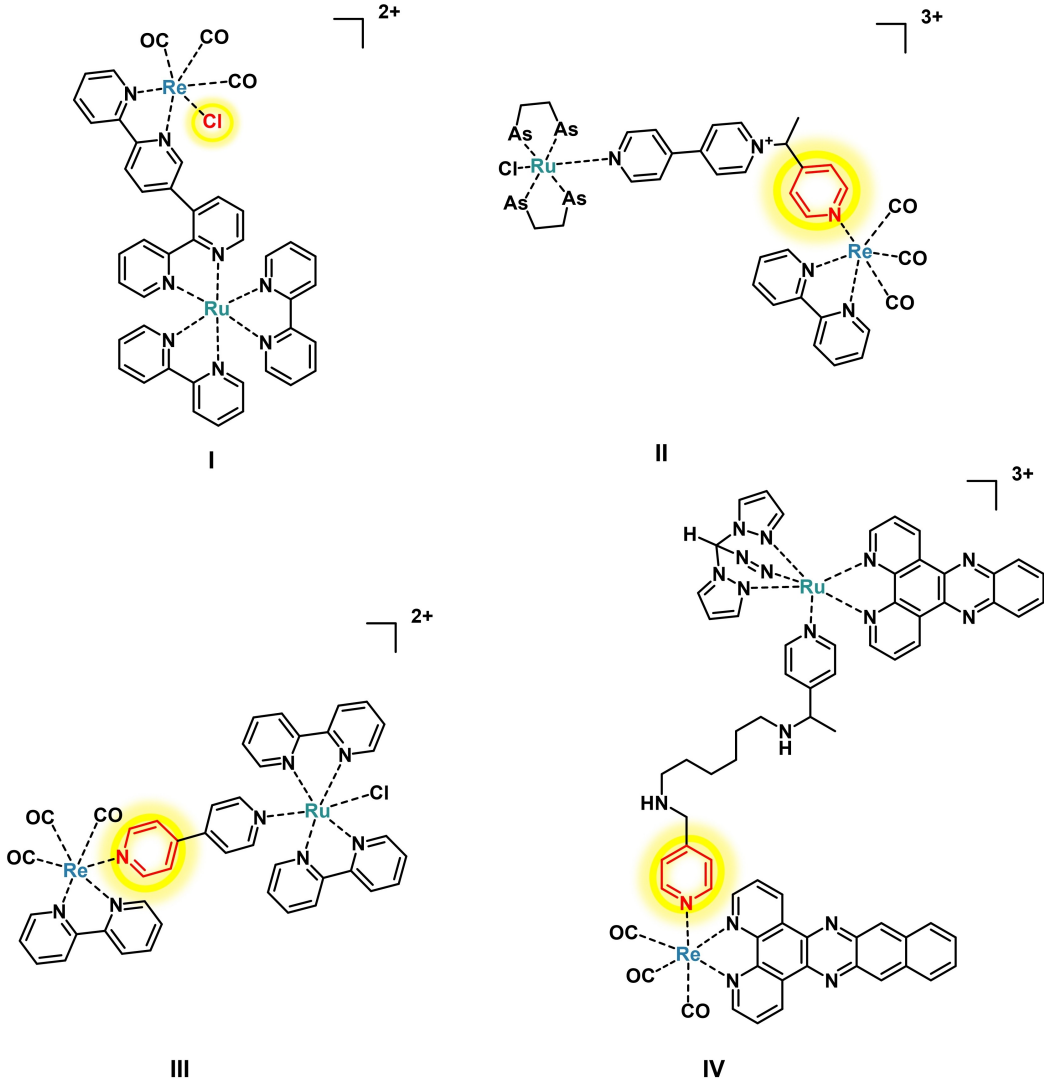

Figure 1. Representative structures of Ru–Re bimetallic complexes where the Re is bound by a bidentate ligand and either a halogen- (Cl) or a monodentate ligand (pyridine).[23–26]

which are rarely used in biological fields. Recently, Re(dppz)$(CO)_3$ based Ru compound (**IV**) displayed a significant phototoxicity towards A2740 ovarian cancer cells and selectively accumulated in mitochondria.[26]

With this in mind, in this work, we report the preparation and characterization of the bimetallic complex **5** (see Scheme 1). Importantly, both metal entities would be electronically coupled in order to allow for a potential shift of the absorption spectrum of the resulting complex. To the best of our knowledge, this is the first compound of this class, whose Re atom is coordinated in a tripodal fashion.

Results and Discussion

The synthesis of the Ru(II) complex **3** and the Ru(II)-Re(I) complex **5** investigated in this work is detailed in Scheme 1. Regarding the design of complex **5**, we decided to use 4,7-diphenyl-1,10-phenanthroline (Bphen) as an auxiliary ligand for the ruthenium in order to allow accessing a better light absorption (i.e., absorption at higher wavelength and with higher efficiency), as previously shown by our group.[27–32] Interestingly, the total charge of the binuclear complex could be easily modulated depending on the Re(I) chelator nature, which allows tuning the solubility of the whole complex. For the Re(I)CO_3 chelating part, we turned our attention towards dipicolylamine (DPA). [Re(I)$(CO)_3$DPA] complexes were found to be stable. A strong influence on the ISC within **5** can be expected due to the close proximity of the two metal centers (SOC scales approximately with Z^4r^{-3}, where Z = atomic number and r = distance).[8] Overall, the Bphen ligands together with the overall charge of +3 for complex **5** should provide a well-balanced hydro- and lipo-philicity.

Compound **3** was obtained by refluxing ruthenium precursor Ru(Bphen)$_2$Cl$_2$ (**2**)[33] with the known ligand **1**[34] in MeOH/H_2O (1 : 1) for 15 h and was precipitated as its dihexafluorophosphate salt. This novel Ru(II) complex was then reacted with the tricarbonyl Re(I) salt **4**[35] in MeOH at 80 °C to yield complex **5**,

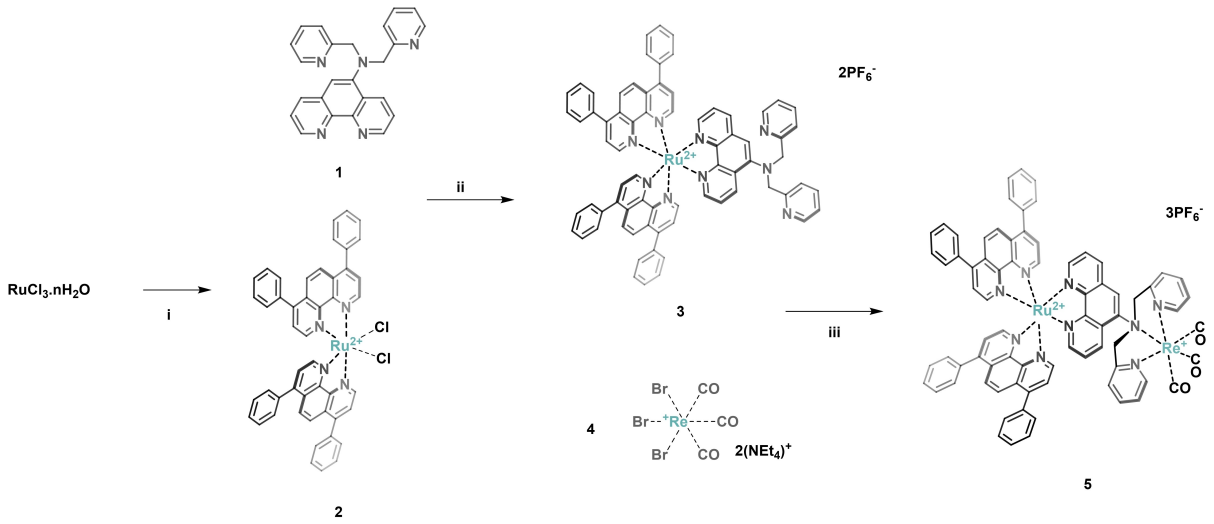

Scheme 1. Synthetic procedures for complexes **3** and **5** (i) Bphen, LiCl, DMF, reflux, 12 h, 85%; (ii) MeOH, H_2O, reflux, 15 h, NH_4PF_6, 44%; (iii) MeOH, reflux,15 h, 69%.

which was also precipitated as its hexafluorophosphate salt. Both complexes were characterized by ^1H, ^{13}C NMR and FT-IR as well as ESI-HRMS (Figures S1–S12). For **5**, the expected carbonyl bands in the IR were observed at 2040 cm^{-1} and 1920 cm^{-1}. Worthy of note, the structure of Ru(II) complex **3** was confirmed by single crystal X-ray crystallography (Figure 2 and Table S1), which grew from acetonitrile/diethyl ether containing a ruthenium(II) dicationic complex, two PF_6^- counterions and two solvents of acetonitrile. One pyridine group is disordered over two sets of positions with site-occupancy factors of 0.143(10) and 0.857(10). One pyridin-2-ylmethyl ligand is also disordered over two sets of positions with site-occupancy factors of 0.273(9) and 0.727(9). The Ru(II) ion is coordinated by two bathophenanthroline ligands and one substitute phenanthroline ligand through the N atoms in a distorted octahedral geometry.

In order to better understand the photophysical properties of complex **3** and complex **5**, the UV-Vis absorption spectrum was recorded (Figure 3a). Compared to $Ru(bpy)_3Cl_2$, complex **3** demonstrated similar distinct photophysical characteristics, which exhibited absorption peaks centered around 290 nm in the UV region, attributed to bipyridine centered transitions. In

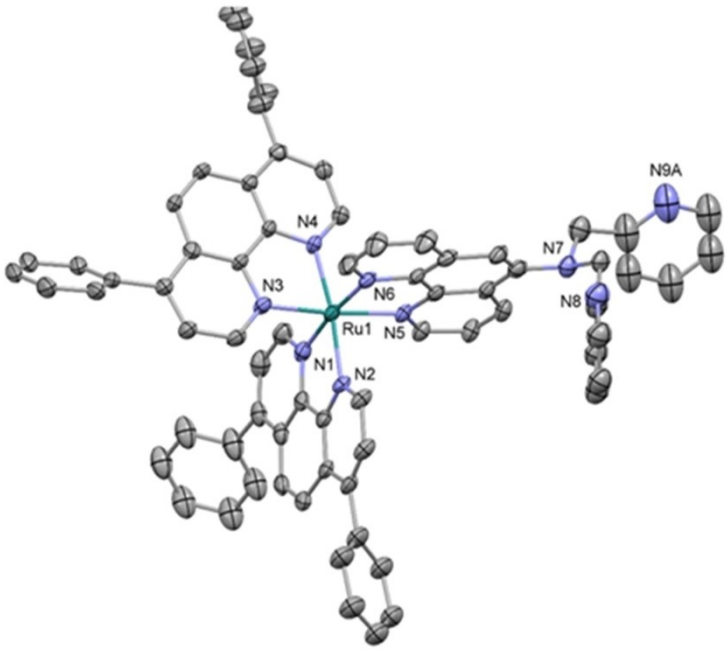

Figure 2. Molecular structure of one of the two dicationic species present in the asymmetric unit of **3**. The disorder and all hydrogen atoms are omitted for clarity.

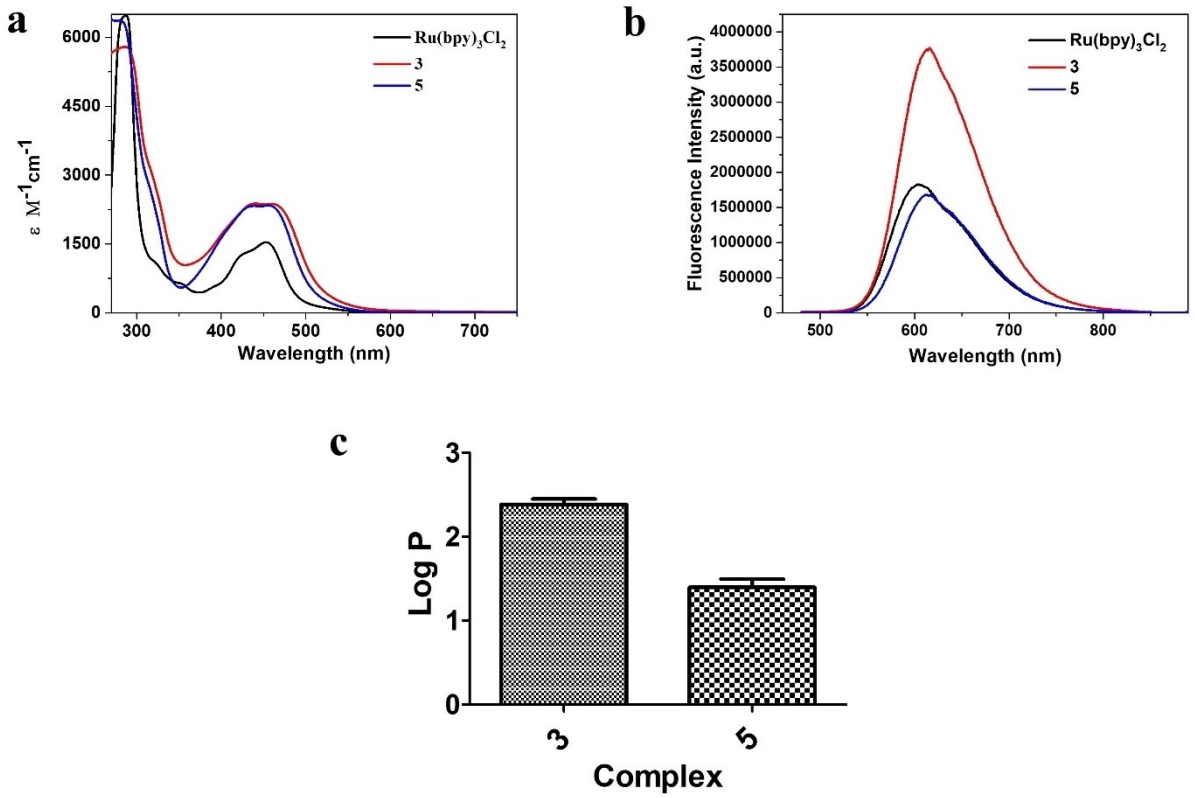

Figure 3. (a) UV-Vis absorption spectra of $Ru(bpy)_3Cl_2$, complex **3** and complex **5**. The spectra were recorded in water at a concentration of 50 μM; (b) Emission spectra of $Ru(bpy)_3Cl_2$, complex **3** and complex **5**. The spectra were recorded in water at a concentration of 50 μM (Excitation:450 nm, slit: 6 nm); (c) Octanol/PBS partition coefficients of complex **3** and complex **5**.

the visible region, it displayed an absorption band characteristic of metal to ligand charge transfer (MLCT) centered around 450 nm. The emission spectrum of complex **3** ranges from approximately 540 to 800 nm, indicating its emission properties in the red to near-infrared region (NIR). Complexation with the rhenium did not seem to strongly affect the absorption of the complex as the UV spectrum for complex **5** did not showcase any major differences (see Figure S14). However, an important decrease in the fluorescence intensity was observed (Figure 3b). In order to gain a deeper understanding of the photophysical properties, a series of photostability experiments were conducted using PBS and acetonitrile as solvents. The results (detailed in the Figure S13), revealed that compound **3** demonstrated a relatively stable behavior when exposed to 540 nm irradiation. To assess the effect of the overall charge on the hydrophilicity of complexes, their partition coefficient between PBS and octanol (LogP) was determined (see Figure 3c). Compound **5** demonstrated an improved partition in PBS in comparison to compound **3**, thanks to the presence of the Re moiety, which suggested that the overall charge of +3 of compound **5** could provide an interesting hydro- and lipophilicity balance.

During the analysis of compound **5**, we discovered that its stability in solution was far from ideal. Therefore, its stability was first investigated by ^1H NMR spectroscopy by recording ^1H spectra in CD_3CN at different time points. **3** has a characteristic singlet peak at 4.80 ppm in CD_3CN (Figure 4a), which can be ascribed to the four H atoms of the two CH_2 groups of the DPA chelator. Due to the linkage of N to Re, the two CH_2 groups of **5** displayed distinct shifts at 5.33 and 5.76 ppm, respectively (Figure 4b). However, when **5** was placed in CD_3CN for 12 h, some changes occurred in the NMR spectrum, with three peaks appearing in the same region (5.34 and 5.76 ppm belong to **5**, 4.72 ppm belong to **3**, Figure 4c). Furthermore, the integral ratio of CH_2 in complex **3** and CH_2 of complex **5** is 1:5.2, it proves that 16% of complex **5** was transformed into complex **3** after 12 h, which suggested that there are some issues with the stability of **5** with regards to the Re(I) complexation, which can be slowly converted back to **3** if kept in solution.

In order to have further insight into the stability of **5**, HPLC was used to monitor the stability of complexes **3** and **5**. The retention time of **3** is 11.369 min (Figure 5a) while the one of **5** is 10.456 min (Figure 5b). Some degradation of compound **5** in CH_3CN was indeed observed after 16 h, as indicated by the appearance of a peak 11.269 min (Figure 5c). To ascertain that the measured peak was actually **3**, pure **3** was added to the solution, which confirmed our hypothesis (Figure 5d). Furthermore, after analyzing the integrated areas of 10.395 and 11.268 in Figure 5c and Table S2, it was demonstrated that ca. 20% of compound **5** was converted into compound **3** after 16 h. Overall, this additional experiment suggests that **5** is not very stable and is slowly converted by to **3** in solution. This observation is consistent with that observed by NMR.

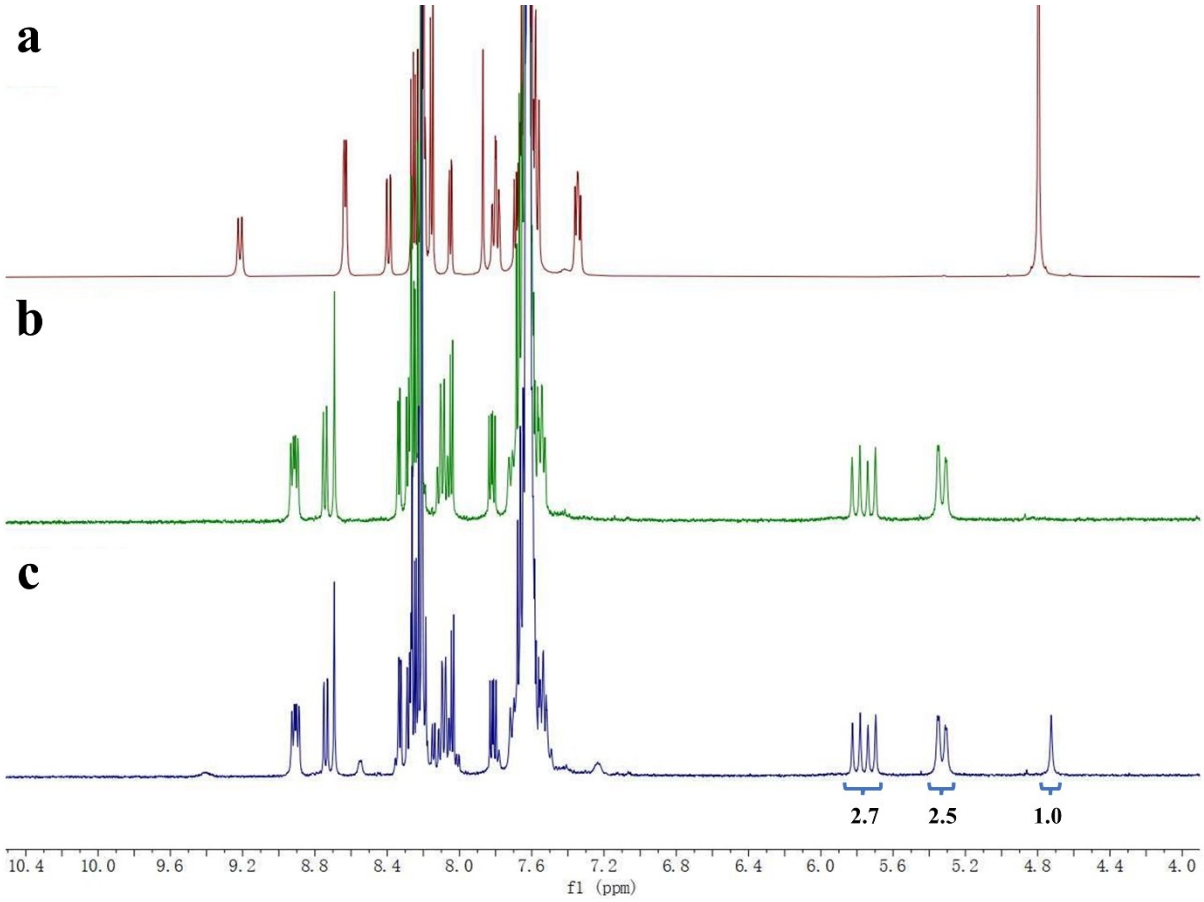

Figure 4. ^{1}H NMR spectra of **3** (a); **5** (b) and **5** after 12 h in CD_3CN (c).

Due to the stability issue of **5**, we decided to only test the biological activity of **3**. The phototoxicity of complex **3** was assessed by incubating the complex with human lung carcinoma A549 and human colon colorectal adenocarcinoma HT29 cells, as well as non-cancerous retinal pigment epithelium RPE1 cells. After incubation, the cells were irradiated with light at a wavelength of 540 nm for 40 minutes. Additionally, the toxicity of the complex in the absence of light (dark condition) was evaluated by incubating the cells with the complex for 4 hours without subsequent light exposure. The phototoxicity index (PI) is derived from the ratio of the IC_{50} (concentration that causes 50% cell death) in the dark to the IC_{50} following light irradiation. It quantifies the relative increase in cell-killing effectiveness of the complex when exposed to light. Protoprophyrin IX (PPIX), a clinically-approved PDT PS, was used as the positive control for comparison purposes. As shown in Table 1 and Figure S15-17, complex **3** was found to be non-toxic in the dark (>100 μM). However, complex **3** exhibited notable and comparable phototoxicity against cancer cell lines HT29 and A549, with submicromolar IC_{50} values of 0.39 μM and 0.74 μM, respectively. These values were 6 to 12 times lower than the phototoxic IC_{50} value observed on the normal cell line RPE1, indicating a favorable selectivity towards cancer cells. Very interestingly, complex **3** was significantly more phototoxic to cancer cells than PPIX, while less phototoxic to normal cells. The PI values of 135.2 for A549 and 256.4 for HT29 are interesting. These results highlight the promising photodynamic properties of complex **3** for targeting cancer cells.

Table 1. Cytotoxicity (IC_{50}, μM) of Complex **3** in comparison with PPIX against cancerous A549/HT29 cells and non-cancerous RPE1 cells after 4 h of incubation; under irradiation (540 nm,1.2 mW, 40 min) or in the dark.

		PPIX	Complex **3**
A549	dark	>100	>100
	light	1.24 ± 0.60	0.74 ± 0.13
	PI	80.6	135.1
HT29	dark	>100	>100
	light	3.41 ± 1.38	0.39 ± 0.02
	PI	29.3	256.4
RPE1	dark	>100	>100
	light	2.21 ± 0.49	4.46 ± 0.47
	PI	45.2	22.4

[a] Standard deviation, $PI = IC_{50}^{dark}/IC_{50}^{light}$.

These very exciting results prompted us to further investigate the internalization mechanism of complex **3**. Its subcellular localization was determined by confocal microscopy using the intrinsic luminescence of Ru(II) compound. A549 cells were co-incubated with complex **3** for 4 h, followed by the

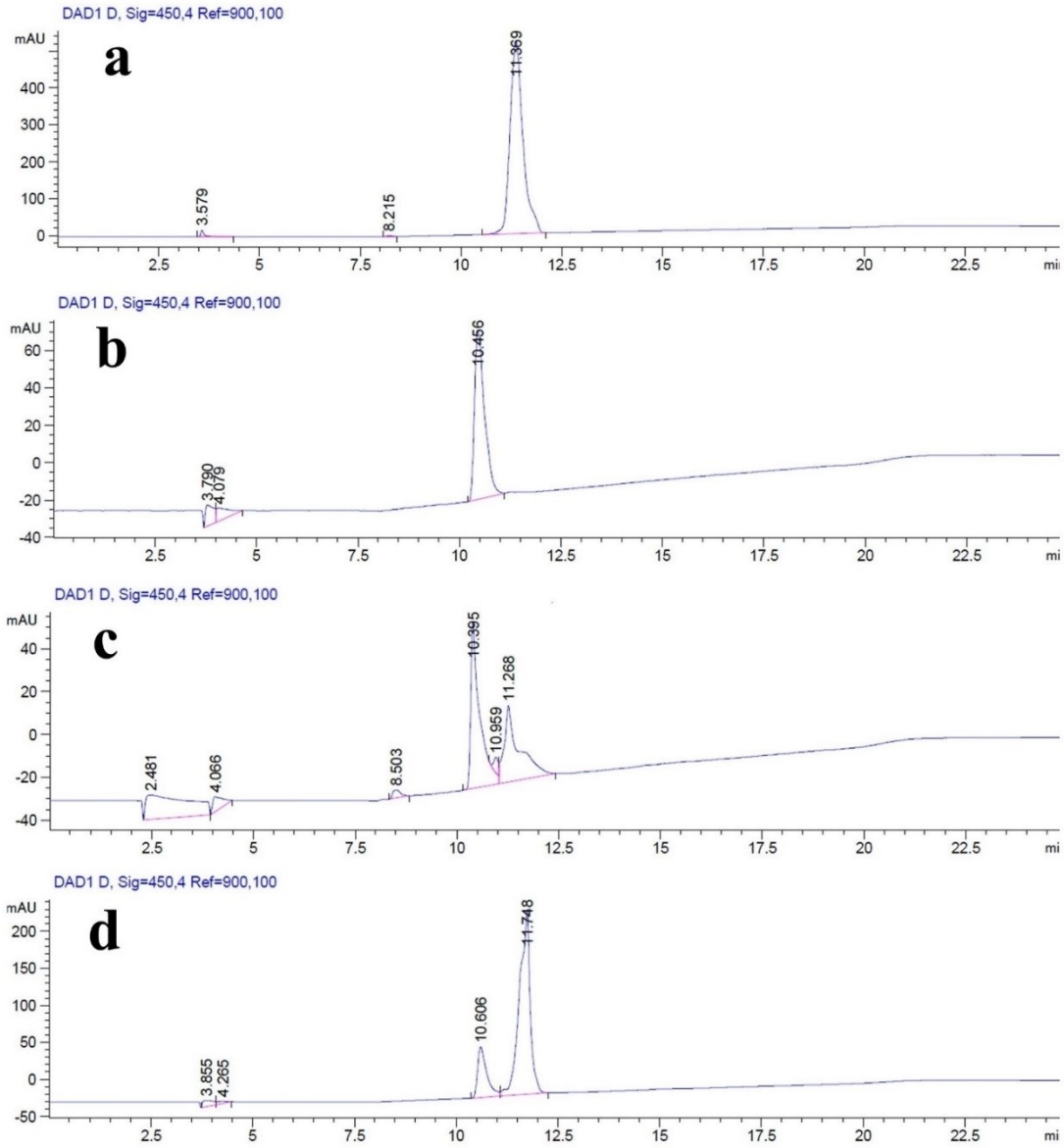

Figure 5. HPLC chromatogram of **3** (a); **5** (b); **5** in acetonitrile after 12 h (c) and the mixture of **5** after 12 h and **3** (d). The solvents (HPLC grade) were acetonitrile (MeCN) (solvent A) and millipore water (solvent B). The HPLC gradients used are as follows: 0–3 min: isocratic 95% B (5% A); 3–17 min: linear gradient from 95% B (5% A) to 0% B 100% A); 17–23 min: isocratic 0% B (100% A); 23–25 min: linear gradient from 0% B (100% A) to 95% B (5% A). The flow rate was 1 mL/min. Detection was performed at 450 nm with a slit of 4 nm.

addition of a cell membrane targeting tracker (Green Mask) and a mitochondrial targeting tracker (MTG). This allowed for monitoring the localization of the compound within the cells. The results depicted in Figure 6 and Figure S18 clearly indicated internalization of complex **3** within the cells. The colocalization coefficients between complex **3** and the cell membrane/mitochondria were measured as 0.14 and 0.59, respectively. These coefficients suggested that compound **3** primarily localized within the mitochondria of the cells.

Conclusions

In this work, we designed and characterized a Ru(II) complex **3** that bears a dipicolylamine moiety to allow chelation of a second metallic center. The Ru(II)-Re(I) complex **5** was thus prepared and characterized. During the course of this work, we found out that this dimetallic complex did not exhibit suitable stability in solution for use in biological systems as decoordination of the rhenium was observed. Yet, the parent Ru(II) complex (**3**) itself was further studied in terms of its biological activity. Complex **3** demonstrated selective phototoxicity towards A549 and HT29 cancer cells compared to normal cells, with excellent phototoxicity indexes that surpass those of the approved drug PPIX. This complex was also found to localize

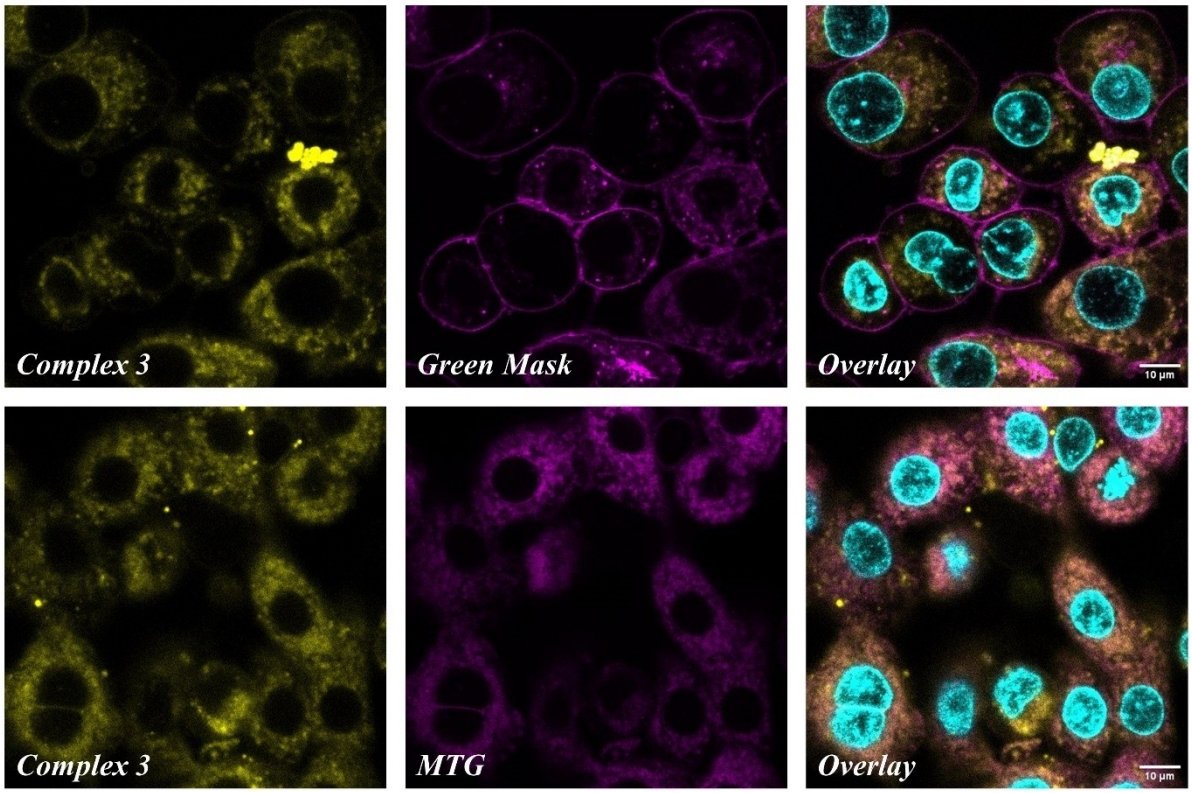

Figure 6. Confocal microscopy images of A549 cells incubated with complex **3** (5 μM, 4 h) and co-labeled with Green Mask (100 nM, 10 min) or MTG (100 nM, 10 min). Hoechst 33342 was excited at 405 nm; complex **3**, Green Mask and MTG were excited at 488 nm. The luminescence was collected at 405/420-450 nm (Hoechst), 488/670-800 nm (complex **3**), and 488/500-550 nm (Green Mask and MTG), respectively.

preferentially in the mitochondria, an organelle that plays a crucial role in various cellular processes. These findings provide valuable insights into the development of targeted photosensitizers for photodynamic therapy and in particular pave the way for further studies to investigate: 1. the role of the dipicolylamine moiety in the biological properties of **3** and 2. the possibility to construct more stable bimetallic scaffolds using this chelating moiety.

Experimental Section

Materials

Ruthenium trichloride x-hydrate was provided by I^2CNS (Zurich); 4,7-diphenyl-1,10-phenanthroline(Bphen), lithium chloride(anhydrous,99%) and ammonium hexafluorophosphate were obtained from Alfa Aesar. Diglyme, bromopentacarbonylrhenium(I) and 2-(bromomethyl)pyridine hydrobromide were purchased from Sigma-Aldrich. 1,10-phenanthroline-5-amine, sodium hydride (in paraffin 60%) were purchased from TCI. All solvents were purchased of analytical or HPLC grade from VWR, and solvents for reactions were of pro analysis (p.a.) grade or distilled prior to their use.

Instruments and methods

^{1}H nuclear magnetic resonance (^{1}H NMR) spectra were determined on a Bruker AV 400 or 500 MHz spectrometer. High-resolution ESI mass spectrometry (HR ESI-MS) spectra were recorded on an LTQ-Orbitrap XL from Thermo Scientific. Infrared Spectroscopy was obtained on a SpectrumTwo FT-IR Spectrometer (Perkin-Elmer) equipped with a Specac Golden GateTM ATR (attenuated total reflection) accessory, applied as neat samples, $1/\lambda$ in cm^{-1}. Analytical HPLC measurement was performed using a 1260 Infinity HPLC System (Agilent Technology) comprising: 2 x Agilent G1361 1260 Prep Pump system with an Agilent G7115 A 1260 DAD WR Detector equipped with an Agilent Pursuit XRs 5 C18 (100 Å, C18 5 μm 250×4.6 mm) Column and an Agilent G1364B 1260-FC fraction collector. The solvents (HPLC grade) were acetonitrile (MeCN) (solvent A) and millipore water (solvent B). The HPLC gradients used are as follows: 0–3 min: isocratic 95% B (5% A); 3–17 min: linear gradient from 95% B (5% A) to 0% B 100% A); 17–23 min: isocratic 0% B (100% A); 23–25 min: linear gradient from 0% B (100% A) to 95% B (5% A). The flow rate was 1 mL/min. Detection was performed at 215 nm, 250 nm, 350 nm, 450 nm, 550 nm, and 650 nm with a slit of 4 nm. UV-Vis spectra were recorded on Cary 4000 UV-Vis spectrometer (Agilent) and in 96 well plates with a SpectraMax M2 Spectrometer (Molecular Devices) or with a Varian Cary 8454″ UV/Visible spectrophotometer and quartz cuvettes (width 1 cm); Fluorescence spectra were measured by a Horiba FluoroMax Spectrofluorometers.

Synthesis and characterization

N,N-bis(pyridin-2-ylmethyl)-1,10-phenanthrolin-5-amine (1)

Phen-DPA (**1**) was synthesized following a procedure reported by Lee et al.[36] 1,10-phenanthrolin-5-amine (117 mg, 0.60 mmol) and NaH (in paraffin 60%, 289 mg, 7.22 mmol) were suspended in THF (25 mL) in an ice bath under an inert atmosphere of nitrogen for 1 h. 2-(bromomethyl)pyridine hydrobromide(608 mg, 2.41 mmol) was slowly added and the mixture was further stirred for 48 h at room temperature, and the reaction was quenched by slow addition of water (10 mL). The product was extracted with CH_2Cl_2 (30 mL x 2), and the organic layer was washed with H_2O (20 mL*2), dried over $MgSO_4$, and evaporated to dryness. The residual solid was purified by column chromatography on silica gel, and the product was eluted with CH_2Cl_2/MeOH (20:1 to 1:2, v/v) and subsequently isolated as a brown solid ($R_f = 0.21$, CH_2Cl_2/MeOH = 1:1). Yield: 54.4 mg (24%, 80% purities). ^{1}H NMR (400 MHz, methanol-d_4): δ 9.15 (dd, J = 8.3, 1.7 Hz, 1H), 9.04 (dd, J = 4.4, 1.7 Hz, 1H), 8.87 (dd, J = 4.4, 1.7 Hz, 1H), 8.42 (ddd, J = 5.0, 1.8, 0.9 Hz, 2H), 8.14 (dd, J = 8.2, 1.7 Hz, 1H), 7.81–7.76 (m, 1H), 7.65 (td, J = 7.7, 1.8 Hz, 2H), 7.60–7.56 (m, 1H), 7.48 (dt, J = 7.9, 1.1 Hz, 2H), 7.38 (s, 1H), 7.20 (ddd, J = 7.6, 5.0, 1.2 Hz, 2H), 4.59 (s, 4H). HR ESI-MS calculated: m/z = 378.1713 (M^+), found: m/z = 378.1714 (M^+). *The data are in accordance with the literature.*

[Ru(Bphen)$_2$Cl$_2$] (2)

$Ru(phen)_2Cl_2$ was synthesized using a reported protocol.[33] A mixture of Ruthenium trichloride x-hydrate (0.89 g, 3.4 mmol), 4,7-diphenyl-1,10-phenanthroline (Bphen, 2.33 g, 7.0 mmol), and LiCl (1.02 g, 24 mmol) were dissolved in DMF (25 mL) and refluxed while stirring for 12 h. The reaction was then cooled down to room temperature, the solvent was removed by rotary evaporation, and acetone (50 mL) was slowly added. The mixture was then stored at 0 °C overnight for crystallization before filtration. The solid residue was washed with water, acetone, and diethyl ether to afford $[Ru(Bphen)_2Cl_2]$ as a black-purple solid, directly used in the next step without separation. Yield: 85%

[Ru(Bphen)$_2$phen-DPA](PF$_6$)$_2$ (3)

The complex $[Ru(Bphen)_2phen\text{-}DPA](PF_6)_2$ was synthesized in the same way as reported protocols.[27] **2** (163 mg,0.2 mmol) and **1** (76 mg, 0.2 mmol) were suspended in a degassed water/MeOH mixture (1:1) (20 mL) and refluxed for 15 h, resulting in a deep red solution. The solution was cooled to room temperature and a few drops of saturated NH_4PF_6 aqueous solution were added while stirring, forming a red precipitate. After filtration, the crude solid was purified by chromatography on silica using a system of CH_3CN/H_2O/KNO_3 (100:4:1 to 5:1:0.25) as the eluent. ($R_f = 0.36$, CH_3CN/H_2O/KNO_3 = 5:1:0.25) The solvent was removed in vacuo and the red-coloured residue was washed several times with water, pentane and diethyl ether to give **3** as a red solid (127 mg, 0.09 mmol, 44%).^{1}H NMR (400 MHz, Acetonitrile-d_3) δ 9.30–9.18 (m, 1H), 8.64 (dd, J = 5.0, 1.6 Hz, 2H), 8.46–8.39 (m, 1H), 8.32–8.15 (m, 9H), 8.06 (dd, J = 5.2, 1.3 Hz, 1H), 7.94–7.76 (m, 3H), 7.74–7.53 (m, 28H), 7.36 (ddd, J = 7.6, 5.0, 1.2 Hz, 2H), 4.81 (s, 4H). ^{13}C NMR (101 MHz, Acetonitrile-d_3) δ 157.8, 153.6, 153.4, 153.3, 153.1, 151.8, 150.1, 150.0, 149.9, 149.5, 149.4, 148.1, 146.2, 139.2, 136.7, 136.3, 134.9, 131.8, 130.7, 130.6, 129.9, 127.0, 126.9, 126.3, 124.5, 124.2, 117.1, 59.4. ESI-HRMS (pos. detection mode): calculated for $C_{72}H_{51}N_9Ru$ $[M\text{-}2PF_6]^{2+}$ m/z 571.6650; found: 571.6663. HPLC: 0–3 min: isocratic 5% millipore water (95% acetonitrile); 3–17 min: linear gradient from 5% A (95% B) to 100%A (0% B); 17–23 min: isocratic 100% A (0% B), 23–25 min: linear gradient from 100% A (0% B) to 5% A (95% B) T_R = 11.650 min. Elemental analysis calculated for $C_{72}H_{51}F_{12}N_9P_2.3.5H_2O$. CH_3CN (%): C 57.81; H 4.00; N 9.11; found: C 57.55, H 3.67, N 9.21. IR (cm^{-1}): 3670, 3590, 3090, 3070, 2500, 2170, 2030, 1970, 1630, 1590, 1560, 1510, 1480, 1420, 1400, 1300, 1260, 1220, 1180, 1160, 1130, 1100, 1050, 1030, 1020, 1000, 970, 930, 830, 760, 730, 700,670, 650.

[NEt$_4$]$_2$[ReBr$_3$(CO)$_3$]

The precursor $[NEt_4]_2[ReBr_3(CO)_3]$ (**4**) was synthesized following a known procedure.[35] A mixture of $ReBr(CO)_5$ (0.5 g, 1.23 mmol) and $(NEt_4)Br$ (0.52 g, 2,47 mmol) was suspended in diglyme (25 mL) and heated to 115 °C for 72 h. After cooling to room temperature, the solid was filtrated and washed several times with diglyme (20 mL) and Et_2O (50 mL). After drying under vacuo, complex **4** was obtained as a yellow solid (0.673 g, 71%). Spectroscopic data (IR) were in agreement with the literatures. Elemental analysis calculated for $C_{19}H_{40}Br_3N_2O_3Re$ (%): C 29.60; H 5.25; N 3.65; found: C 29.61, H 5.00, N 3.65. IR (cm^{-1}) : 2990, 2000, 1870, 1580, 1460, 1400, 1370, 1310, 1180, 1030, 1000, 800, 650.

[Ru(Bphen)$_2$phen-DPA]Re(CO)$_3$(PF$_6$)$_2$ (5)

Complex **5** $[Ru(Bphen)_2phen\text{-}DPA]Re(CO)_3(PF_6)_2$ was synthesized by dissolving **3** (50 mg, 0.034 mmol) and **4** (18.8 mg, 0.034 mmol) in MeOH (15 mL) and heated to 80 °C for 15 h. After the whole consumption of **3** (checked by HPLC), the reaction was cooled to room temperature and saturated NH_4PF_6 aqueous solution was added to the mixture. The solvent was removed in vacuo and the red residue was washed several times with water, Et_2O and pentane to give **5** as a red solid (40 mg, 0.023 mmol, 69%) ($R_f = 0.45$, CH_3CN/H_2O/KNO_3 = 5:1:0.25).

^{1}H NMR (400 MHz, Acetonitrile-d_3) δ 8.92 (t, J = 6.8 Hz, 2H), 8.78–8.68 (m, 2H), 8.39–8.18 (m, 10H), 8.16–8.04 (m, 3H), 7.83 (dd, J = 8.3, 5.3 Hz, 2H), 7.79–7.50 (m, 28H), 5.78 (dd, J = 38.6, 17.1 Hz, 2H), 5.35 (d, J = 17.1 Hz, 2H). ^{13}C NMR (101 MHz, Acetonitrile-d_3) δ 195.8, 195.6, 194.4, 154.7, 154.3, 153.6, 153.5, 153.3, 153.2, 150.9, 150.2, 149.4, 149.1, 148.3, 142.2, 138.1, 136.6, 135.0, 130.8, 130.6, 130.1, 128.1, 127.7, 127.6, 127.3, 127.0, 125.9, 125.5, 125.3, 70.8. ESI-HRMS (pos. detection mode): calculated for $C_{75}H_{51}N_9O_3RuRe$ $[M\text{-}3PF_6]^{3+}$ m/z 471.4233; found: 471.4241. HPLC: 0–3 min: isocratic 5% millipore water (95% acetonitrile); 3–17 min: linear gradient from 5% A (95% B) to 100%A (0% B); 17–23 min: isocratic 100% A (0% B), 23–25 min: linear gradient from 100% A (0% B) to 5% A (95% B) T_R = 10.701 min. IR (cm^{-1}): 3650, 3590, 3080, 2930, 2860, 2370, 2320, 2170, 2100, 2040, 1920, 1630, 1610, 1600, 1560, 1520, 1490, 1450, 1420, 1400, 1370, 1360, 1310, 1300, 1260, 1230, 1160, 1120, 1090, 1080, 1040, 1030, 1000, 980, 920, 830, 760, 750, 710, 670, 650.

X-ray diffraction study

A single crystal of compound **3** was analysed by X-ray diffraction at 160(1) K on a Rigaku OD XtaLAB Synergy, Dualflex, Pilatus 200 K diffractometer using a single wavelength X-ray source (Cu K_α radiation: λ = 1.54184 Å) from a micro-focus sealed X-ray tube and an Oxford liquid-nitrogen Cryostream cooler. The selected suitable crystal was mounted using polybutene oil on a flexible loop fixed on a goniometer head and immediately transferred to the diffractometer. Pre-experiment, data collection, data reduction, and analytical absorption correction[37] were performed with the program suite *CrysAlisPro*.[38] Using *Olex2*,[39] the structure was solved with the SHELXT[40] small molecule structure solution program and refined with the *SHELXL2018/3* program package[41] by full-matrix

least-squares minimization on F.[38] *PLATON*[42] was used to check the result of the X-ray analysis. Deposition Number 2269280 contains the supplementary crystallographic data for this paper. These data are provided free of charge by the joint Cambridge Crystallographic Data Centre and Fachinformationszentrum Karlsruhe Access Structures service.

Octanol/water partition coefficient (log $P_{o/w}$) measurements

Octanol/water partition coefficients (log $P_{o/w}$) were determined at room temperature following a reported method.[43–44] Octanol (1 mL) and PBS (1 mL) were mixed by continuous shaking at room temperature for 24 h. The complexes (50 μM) were then dissolved in 1 mL octanol, and the same volume of PBS was added. The mixture was continually agitated for another 24 h before the two layers are separated after settling down. The concentrations of the complex in the two phases were measured by UV-Vis spectroscopy.

Cell culture

Human lung carcinoma (A549) cells were grown using F12 media, human colon colorectal adenocarcinoma (HT29) cells were used by McCoy's 5 A Medium, and retinal pigment epithelium (RPE1) cells using DMEM/F-12 medium supplemented with 10% FBS and 1% Penstrep. The cells were cultivated and maintained in a cell culture incubator at 37 °C with 5% CO_2 and 20% O_2 atmosphere. Before an experiment, the cells were passaged three times.

Phototoxicity

The phototoxicity of the complexes was assessed by measuring the cell viability using a fluorometric resazurin assay. The cultivated cells were seeded in sextuplicate in 96 well plates with a density of 4000 cells per well in 100μL of media. After 24h, the medium was removed and the cells were treated with increasing concentrations of the complex diluted in cell media achieving a total volume of 100 μL at 37 °C with 5% CO2 and 20% O2 atmosphere for 4 h. Then the media was replaced with 100 μL fresh medium, plates were irradiated at light wavelength (540 nm for 40 min (light dose 1.2 mW) at 37 °C using a LUMOS-BIO photoreactor (Atlas Photonics). As a control, a plate was kept in the dark for 40 min at the same condition. Then cells were cultivated for another 44 h, the media was changed with fresh media containing resazurin with a final concentration of 0.2 mg/mL. After 4 h of incubation at 37 °C, the fluorescence signal of resorufin product was measured (λ_{ex}: 540 nm and λ_{em}: 590 nm) in a BioTek®. IC_{50} values were then calculated using GraphPad Prism software. Each experiment was performed in duplicate and an average IC_{50} value (in μM) was reported with a standard deviation.

Cellular uptake

CT26 cells (1×10^5 cells) were seeded in 35 mm culture dishes for 24 h. Cell medium was then replaced by fresh medium containing 5 μM of **Complex 3**. After incubation for 4 h in the dark at 37 °C, cells were washed with PBS. Cells were then stained with Hoechst 33342 (1 μg/mL), and Green Mask (100 nM) or MTG (100 nM) at room temperature for 10 min. Live cells were imaged in a confocal laser scanning microscope (Leica SP8) equipped with an x63/1.40 plan apochromat objective. The excitation/emission wavelengths were 405/420–450 nm (Hoechst), 488/670-800 nm (Complex **3**), and 488/500-550 nm (Green Mask and MTG). Care was taken to use laser intensities as low as possible to avoid any phototoxicity.

Acknowledgements

This work was financially supported by an ERC Consolidator Grant PhotoMedMet to G.G. (GA 681679), by the ANR (COSETTE project) and has received support under the program *Investissements d'Avenir* launched by the French Government and implemented by the ANR with the reference ANR-10-IDEX-0001-02 PSL (G.G.). Y. W. thanks the China Scholarship Council for financial support. Financial support by the Austrian Science Fund (FWF) is acknowledged (grant number I5721-N to T.L.M).

Conflict of Interests

There are no conflicts to declare.

Data Availability Statement

The data that support the findings of this study are available in the supplementary material of this article.

Keywords: bioinorganic chemistry · metals in medicine · photodynamic therapy · Rhenium(I) complex · Ruthenium(II) complex

[1] P. Agostinis, K. Berg, K. A. Cengel, T. H. Foster, A. W. Girotti, S. O. Gollnick, S. M. Hahn, M. R. Hamblin, A. Juzeniene, D. Kessel, *Ca-Cancer J. Clin.* **2011**, *61*, 250–281.
[2] F. Heinemann, J. Karges, G. Gasser, *Acc. Chem. Res.* **2017**, *50*, 2727–2736.
[3] S. A. McFarland, A. Mandel, R. Dumoulin-White, G. Gasser, *Curr. Opin. Chem. Biol.* **2020**, *56*, 23–27.
[4] M. Jakubaszek, B. Goud, S. Ferrari, G. Gasser, *Chem. Commun.* **2018**, *54*, 13040–13059.
[5] A. Gandioso, K. Purkait, G. Gasser, *Chimia* **2021**, *75*, 845–855.
[6] S. Monro, K. L. Colon, H. Yin, J. Roque, 3rd, P. Konda, S. Gujar, R. P. Thummel, L. Lilge, C. G. Cameron, S. A. McFarland, *Chem. Rev.* **2019**, *119*, 797–828.
[7] J. Kou, D. Dou, L. Yang, *Oncotarget* **2017**, *8*, 81591.
[8] C. M. Marian, *Wiley Interdiscip. Rev.: Comput. Mol. Sci.* **2012**, *2*, 187–203.
[9] J. Zou, Z. Yin, K. Ding, Q. Tang, J. Li, W. Si, J. Shao, Q. Zhang, W. Huang, X. Dong, *ACS Appl. Mater. Interfaces* **2017**, *9*, 32475–32481.
[10] T. Wang, Y. Hou, Y. Chen, K. Li, X. Cheng, Q. Zhou, X. Wang, *Dalton Trans.* **2015**, *44*, 12726–12734.
[11] M. Ucuncu, E. Karakus, E. Kurulgan Demirci, M. Sayar, S. Dartar, M. Emrullahoglu, *Org. Lett.* **2017**, *19*, 2522–2525.
[12] P. S. Felder, S. Keller, G. Gasser, *Adv. Ther.* **2020**, *3*, 1900139.
[13] A. Leonidova, G. Gasser, *ACS Chem. Biol.* **2014**, *9*, 2180–2193.
[14] P. Collery, F. Santoni, J. Ciccolini, T. N. N. Tran, A. Mohsen, D. Desmaele, *Anticancer Res.* **2016**, *36*, 6051–6057.
[15] Q. Qi, Q. Wang, Y. Li, D. Z. Silva, M. E. L. Ruiz, R. Ouyang, B. Liu, Y. Miao, *Molecules* **2023**, *28*, 2733.
[16] E. B. Bauer, A. A. Haase, R. M. Reich, D. C. Crans, F. E. Kühn, *Coord. Chem. Rev.* **2019**, *393*, 79–117.
[17] C. C. Konkankit, S. C. Marker, K. M. Knopf, J. J. Wilson, *Dalton Trans.* **2018**, *47*, 9934–9974.
[18] A. Leonidova, V. Pierroz, R. Rubbiani, J. Heier, S. Ferrari, G. Gasser, *Dalton Trans.* **2014**, *43*, 4287–4294.
[19] X. Su, W. J. Wang, Q. Cao, H. Zhang, B. Liu, Y. Ling, X. Zhou, Z. W. Mao, *Angew. Chem. Int. Ed.* **2022**, *61*, e202115800.
[20] S. Van Wallendael, D. P. Rillema, *Coord. Chem. Rev.* **1991**, *111*, 297–318.
[21] M. a. G. Mellace, F. Fagalde, N. E. Katz, *Polyhedron* **2003**, *22*, 369–374.
[22] T. L. Easun, W. Z. Alsindi, M. Towrie, K. L. Ronayne, X.-Z. Sun, M. D. Ward, M. W. George, *Inorg. Chem.* **2008**, *47*, 5071–5078.

[23] R. L. Cleary, K. J. Byrom, D. A. Bardwell, J. C. Jeffery, M. D. Ward, G. Calogero, N. Armaroli, L. Flamigni, F. Barigelletti, *Inorg. Chem.* **1997**, *36*, 2601–2609.
[24] B. J. Coe, N. R. Curati, E. C. Fitzgerald, S. J. Coles, P. N. Horton, M. E. Light, M. B. Hursthouse, *Organometallics* **2007**, *26*, 2318–2329.
[25] M. Velayudham, S. Rajagopal, *Inorg. Chim. Acta* **2009**, *362*, 5073–5079.
[26] H. Saeed, P. J. Jarman, S. Sreedharan, R. Mowll, A. J. Auty, A. A. Chauvet, C. G. Smythe, J. Bernardino de la Serna, J. A. Thomas, *Chem. Eur. J.* **2023**, e202300617.
[27] J. Karges, F. Heinemann, M. Jakubaszek, F. Maschietto, C. Subecz, M. Dotou, R. Vinck, O. Blacque, M. Tharaud, B. Goud, *J. Am. Chem. Soc.* **2020**, *142*, 6578–6587.
[28] J. Karges, F. Heinemann, F. Maschietto, M. Patra, O. Blacque, I. Ciofini, B. Spingler, G. Gasser, *Bioorg. Med. Chem.* **2019**, *27*, 2666–2675.
[29] M. J. Silva, R. Vinck, Y. Wang, B. Saubaméa, M. Tharaud, E. Dominguez-Jurado, J. Karges, P. M. Gois, G. Gasser, *ChemBioChem* **2023**, *24*, e202200647.
[30] R. Vinck, A. Gandioso, P. Burckel, B. Saubaméa, K. Cariou, G. Gasser, *Inorg. Chem.* **2022**, *61*, 13576–13585.
[31] A. Mani, T. Feng, A. Gandioso, R. Vinck, A. Notaro, L. Gourdon, P. Burckel, B. Saubaméa, O. Blacque, K. Cariou, *Angew. Chem. Int. Ed.* **2022**, 135, e202218347.
[32] Z.-Y. Pan, B.-F. Liang, Y.-S. Zhi, D.-H. Yao, C.-Y. Li, H.-Q. Wu, L. He, *Dalton Trans.* **2023**, *52*, 1291–1300.
[33] B. Sullivan, D. Salmon, T. Meyer, *Inorg. Chem.* **1978**, *17*, 3334–3341.
[34] P. K. Lee, W. H. Law, H. W. Liu, K. K. Lo, *Inorg. Chem.* **2011**, *50*, 8570–8579.
[35] R. Alberto, A. Egli, U. Abram, K. Hegetschweiler, V. Gramlich, P. A. Schubiger, *J. Chem. Soc. Dalton Trans.* **1994**, 2815–2820.
[36] P.-K. Lee, W. H.-T. Law, H.-W. Liu, K. K.-W. Lo, *Inorg. Chem.* **2011**, *50*, 8570–8579.
[37] R. Clark, J. Reid, *Acta Crystallogr. Sect. A* **1995**, *51*, 887–897.
[38] M. T. Shool, H. A. Rudbari, T. Gil-Antón, J. V. Cuevas-Vicario, B. García, N. Busto, N. Moini, O. Blacque, *Dalton Trans.* **2022**, *51*, 7658–7672.
[39] O. V. Dolomanov, L. J. Bourhis, R. J. Gildea, J. A. Howard, H. Puschmann, *J. Appl. Crystallogr.* **2009**, *42*, 339–341.
[40] G. M. Sheldrick, *Acta Crystallogr. Sect. A* **2015**, *71*, 3–8.
[41] G. M. Sheldrick, *Acta Crystallogr. Sect. C* **2015**, *71*, 3–8.
[42] A. L. Spek, *Acta Crystallogr. Sect. D* **2009**, *65*, 148–155.
[43] R. Ahmedi, T. Lanez, *J. Fundam. Appl.* **2018**, *10*.
[44] M. Kępczyński, R. P. Pandian, K. M. Smith, B. Ehrenberg, *J. Photochem. Photobiol.* **2002**, *76*.

Manuscript received: June 22, 2023
Revised manuscript received: July 26, 2023
Accepted manuscript online: August 1, 2023
Version of record online: August 11, 2023